Available online at www.sciencedirect.com
SCIENCE DIRECT®
Sensors and Actuators A 107 (2003) 85–95
SENSORS AND ACTUATORS A PHYSICAL
www.elsevier.com/locate/sna

Electromechanical characterisation of dielectric elastomer planar actuators: comparative evaluation of different electrode materials and different counterloads

Federico Carpi [a,*], Piero Chiarelli [a,b], Alberto Mazzoldi [a], Danilo De Rossi [a]

[a] *Interdepartmental Research Center "E. Piaggio", Faculty of Engineering, University of Pisa, via Diotisalvi, 2-56100 Pisa, Italy*
[b] *CNR Institute of Clinical Physiology, Pisa, Italy*

Received June 2002; received in revised form 29 May 2003; accepted 4 June 2003

Abstract

This work intends to extend the electromechanical characterisation of dielectric elastomer actuators. Planar actuators were realised with a 50 μm-thick film of an acrylic elastomer coated with compliant electrodes. The isotonic transverse strain, the isometric transverse stress and the driving current, due to a 2 s high voltage impulse, were measured for four electrode materials (thickened electrolyte solution, graphite spray, carbon grease and graphite powder), four transverse prestress values (19.6, 29.4, 39.2 and 49.0 kPa) and different driving voltages (up to the dielectric breakdown voltage). Results showed that the electrode material and prestress strongly influence the electromechanical performances of the devices. Actuators with graphite spray electrodes and transverse prestress of 39.2 kPa exhibited an isotonic transverse strain of 6% at 49 V/μm, with a driving current per unit electrode area of 3.5 μA/cm^2, and an isometric transverse stress of 49 kPa at 42 V/μm. An electromechanical coupling efficiency of 10% at 21 V/μm was calculated for actuators with thickened electrolyte solution electrodes and a transverse prestress of 29.4 kPa. The presented data permits to choose the best electrode material and the best prestress value (among those tested), to obtain the maximum isotonic transverse strain, the maximum isometric transverse stress or the maximum efficiency for different ranges of applied electric field.

Keywords: Actuator characterisation; Dielectric elastomer; Compliant electrodes

1. Introduction

Since many years, electroactive polymers (EAP) are investigated as compliant, versatile, low density and low cost materials for the satisfaction of the growing need of new actuators for various small scale applications [1–6].

Dielectric elastomers, one particular class of EAP [7], have been demonstrated to be able to generate strains greater than those obtainable with different types of EAP, as well as considerable stresses and low response times [8,9]. They are forecast today as suitable materials to realise high performance devices for the actuation of minirobots, minipumps, loudspeakers, valves and prosthetic devices [9,10].

This article provides an extension of the electromechanical characterisation of planar actuators made of a film of dielectric elastomer coated with compliant electrodes. By applying a voltage difference between the electrodes, the electrostatic forces cause a contraction of the actuator along the electric field direction and an expansion of it along the two orthogonal directions [9]. The principal aim of this work is to evaluate the effect of different compliant electrode materials, different counterloads (prestresses) and different electric fields on the actuator transverse strain (respect to the electric field direction), transverse stress, driving current and electromechanical coupling efficiency.

2. Materials

An acrylic polymer, commercially available as a 50 μm-thick adhesive film (3 M, USA, VHB F9460PC), was used as dielectric elastomer. As shown by the following SEM images, the film presents a regular thickness (Fig. 1) and a quite uniform surface with occasional defects (Fig. 2).

Four electrode materials were tested: graphite spray (Due-ci electronic, Italy, N-77), carbon grease[1] (Chemtron-

* Corresponding author. Tel.: +39-050-554134; fax: +39-050-550650.
E-mail address: carpi@piaggio.ccii.unipi.it (F. Carpi).

[1] Graphite particles suspended in a silicone oil-based grease.

0924-4247/$ – see front matter © 2003 Elsevier B.V. All rights reserved.
doi:10.1016/S0924-4247(03)00257-7

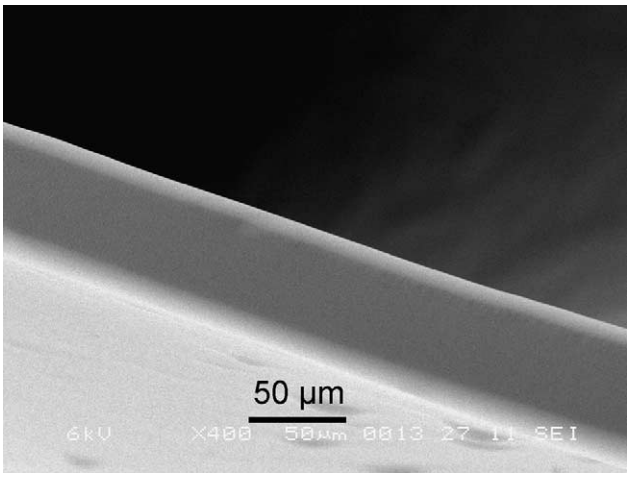

Fig. 1. SEM image showing the film thickness (middle shade of grey).

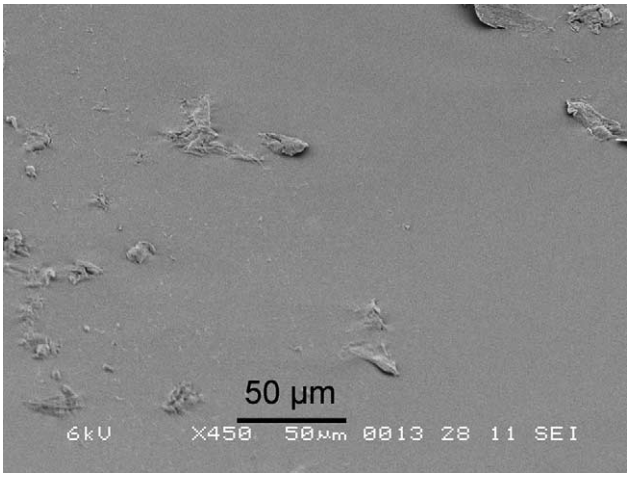

Fig. 2. SEM image showing the film surface seen under a 45° angle out of plane.

ics Circuit Works, USA, CW7200), graphite powder (Zecchi, Italy) and thickened electrolyte solution.[2]

3. Methods

3.1. Sample preparation

Planar actuators were made of rectangular (3 cm × 2 cm) strips of the film coated with the electrode materials, as described below. Carbon grease, graphite powder and thickened electrolyte solution were smeared on the two sides of the strip, while graphite spray electrodes were realised as follows. First of all, the material was sprayed on the same paper support to which the commercial film (previously removed) is coupled; then, after the solvent evaporation, the graphite-covered support was placed in contact with the film and, afterwards, removed again. The film adhesiveness kept the graphite particles stuck to the elastomer, for all the tested deformations of the actuators. This behaviour was found also for graphite powder electrodes, even though the electrodes made of graphite spray showed a superior uniformity, due to the smaller size of the material particles and their more homogeneous distribution, enabled by the mixing solvent.

3.2. Measurements

For each electrode material a two-terminal resistance measurement was performed with a digital multimeter (Keithley, USA, 199 system DMM scanner).

Measurements of actuating properties were carried out placing each actuator in vertical position, constraining its lower end and applying a prestress along the vertical direction (transverse prestress), by connecting its upper end to an appropriate transducer (Fig. 3). Two experimental conditions were realised: isotonic (i.e. at constant load) and isometric (i.e. at constant length), both along the vertical direction, as described below.

In isotonic condition the actuator was connected to an Hall-effect isotonic displacement transducer (Ugo Basile, Italy, 7006). Following the application of an high voltage step impulse (generated by a dc voltage applied for 2 s), the effective driving voltage signal, the driving current signal and the isotonic displacement signal along the vertical direction (transverse displacement) were measured.

In isometric condition the actuator was connected to an isometric force transducer (Ugo Basile, Italy, 7003). In this case, following the application of a 2 s high voltage step impulse, the isometric force signal along the vertical direction (transverse force) was measured.

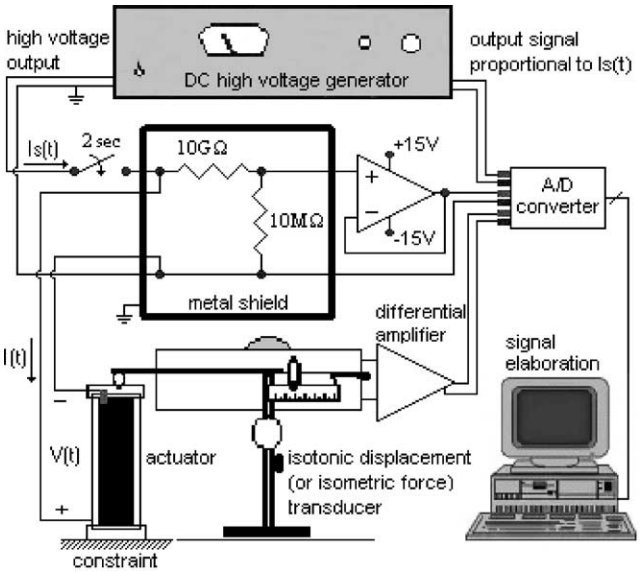

Fig. 3. Experimental set-up.

[2] Proprietary formulation based on an electrolyte (NaCl), thickened agents (polyethylene glycol) and surfactants (sodium laureth sulfate) in water.

Table 1
Mechanical constraints

Applied transverse engineering force (g)	Applied transverse prestress (kPa)	Measured transverse prestrain (%)	Estimated thickness (μm)
2	19.6	19	46
3	29.4	35	43
4	39.2	58	40
5	49.0	83	37

In both isotonic and isometric conditions each signal was measured for the four electrode materials (Section 2), for four transverse prestress values (Table 1) and for different excitation voltages, ranging from 100 V up to the dielectric breakdown voltage of the polymer.

Table 1 lists the transverse (vertical) engineering forces applied on the rest cross-section (2 cm × 50 μm) of the device and the related values of transverse prestress, measured transverse prestrain and estimated thickness, which was calculated as follows. Assuming the thickness direction as the *z*-axis of a Cartesian term *x*, *y*, *z* (Fig. 4), the prestretched thickness (z_0) is given by:

$$z_0 = z_r(1 + S_{zz,p}) \tag{1}$$

where z_r is the rest thickness (50 μm) and $S_{zz,p}$ is the *z* prestrain, which can be estimated by the following relation, assuming a volumetric incompressibility of the polymer [9]:

$$S_{zz,p} = -1 + \frac{1}{\sqrt{1 + S_{xx,p}}} \tag{2}$$

where $S_{xx,p}$ is the measured *x* prestrain (transverse prestrain):

$$S_{xx,p} = \frac{x_0 - x_r}{x_r} \tag{3}$$

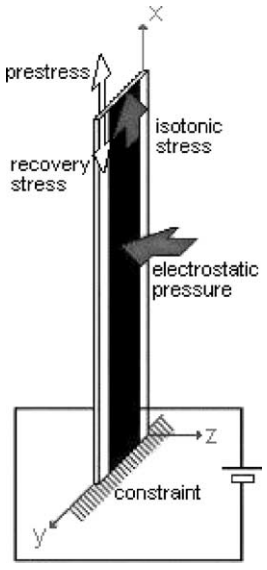

Fig. 4. Planar actuator in isotonic condition.

where x_r (3 cm) and x_0 are respectively the rest and the prestretched length of the actuator.

Fig. 3 shows the experimental set-up: the actuator was connected to a displacement or force transducer and was driven by a dc high voltage generator (Bertan, USA, HV-DC 205A-30P), which, at the same time, gave also an output signal proportional to the supplied current $I_s(t)$ (time (t)). The effective driving voltage signal $V(t)$ was measured by a shielded and buffered voltage divider with an attenuation factor of 10 MΩ/(10 MΩ + 10 GΩ) ≅ 1/1000. The driving current signal $I(t)$ of the actuator was calculated by the difference between the measured supplied current and the calculated current flowing in the voltage divider.

3.3. Simplified analysis of the electrically induced transverse stress

In order to estimate the actuator electromechanical coupling efficiency (Section 3.4), a simplified (first order) analysis of the electrically induced transverse stress, in both isotonic and isometric conditions, was performed as follows.

Assuming the acrylic polymer as a linearly elastic, isotropic and homogenous material with constant volume (Poisson's ratio $\nu = 1/2$ [9]), the mechanical equilibrium of the actuator can be described by the following equations (Hooke's law):

$$S_{xx} = \frac{1}{Y}T_{xx} - \frac{1}{2Y}T_{yy} - \frac{1}{2Y}T_{zz} \tag{4}$$

$$S_{yy} = -\frac{1}{2Y}T_{xx} + \frac{1}{Y}T_{yy} - \frac{1}{2Y}T_{zz} \tag{5}$$

$$S_{zz} = -\frac{1}{2Y}T_{xx} - \frac{1}{2Y}T_{yy} + \frac{1}{Y}T_{zz} \tag{6}$$

where S_{ii} and T_{ii} are respectively the actuator strain and stress along the Cartesian axis i ($i = x, y, z$) and Y is the Young's modulus of the acrylic polymer. By applying an electric field (E_z) along the thickness direction (z), the resulting electrostatic pressure (p) along z is [9]:

$$p = \varepsilon_0 \varepsilon_r E_z^2 \tag{7}$$

where ε_0 is the free-space dielectric permittivity ($\varepsilon_0 = 8.85 \times 10^{-12}$ F/m) and ε_r is the relative dielectric constant of the acrylic polymer.

In the prestress-induced isotonic condition represented in Fig. 4, assuming positive a tensile stress, we have: T_{xx} = prestress, $T_{yy} = 0$, $T_{zz} = -p$. Therefore, the equilibrium strains are expressed by the following equations:

$$S_{xx} = \frac{1}{Y}T_{xx} + \frac{1}{2Y}p \tag{8}$$

$$S_{yy} = -\frac{1}{2Y}T_{xx} + \frac{1}{2Y}p \tag{9}$$

$$S_{zz} = -\frac{1}{2Y}T_{xx} - \frac{1}{Y}p \tag{10}$$

Eq. (8) shows that T_{xx}/Y is the prestress-induced passive isotonic strain along x (transverse prestrain $S_{xx,\mathrm{p}}$), while $p/(2Y)$ is the active isotonic transverse strain, due to the electrostatic pressure. This means that the active isotonic transverse stress along x is:

$$\text{isotonic stress}_{xx} = \frac{p}{2} = \frac{\varepsilon_0 \varepsilon_\mathrm{r} E_z^2}{2} \tag{11}$$

In the isometric condition, realised constraining also the upper end of the actuator, the polymer recovery stress is opposite to the applied prestress. Following the application of an electric field along z, the active isometric transverse stress along x is opposite to the stress (R_x) exerted by the constraining reaction and we have: $S_{xx} = 0$, $T_{xx} = R_x = -(\text{isometric stress}_{xx})$, $T_{yy} = 0$, $T_{zz} = -p$. Therefore, the new equilibrium condition is described by these equations:

$$0 = \frac{1}{Y} T_{xx} + \frac{1}{2Y} p \Rightarrow T_{xx} = -\frac{p}{2} \tag{12}$$

$$S_{yy} = -\frac{1}{2Y} T_{xx} + \frac{1}{2Y} p \Rightarrow S_{yy} = \frac{3p}{4Y} \tag{13}$$

$$S_{zz} = -\frac{1}{2Y} T_{xx} - \frac{p}{Y} \Rightarrow S_{zz} = -\frac{3p}{4Y} \tag{14}$$

Then, the active isometric transverse stress along x is (Eq. (12)):

$$\text{isometric stress}_{xx} = \frac{p}{2} = \frac{\varepsilon_0 \varepsilon_\mathrm{r} E_z^2}{2} \tag{15}$$

Eqs. (11) and (15) show that the isotonic and isometric transverse stresses have the same theoretical expression.

3.4. Calculation of the electromechanical coupling efficiency

A key figure of merit of an electromechanical actuator is represented by its electromechanical coupling efficiency, quantifying the percentage of the supplied electrical energy converted into useful mechanical energy. The efficiency can be defined as:

$$\text{efficiency} = \frac{w_\mathrm{m}}{w_\mathrm{e}} \tag{16}$$

where w_e and w_m are respectively the electric charging work (W_e) and the generated mechanical work (W_m) per unit active volume (Vol) of the prestretched actuator, operating in isotonic condition. These quantities can be calculated as follows:

$$\begin{aligned} w_\mathrm{e} &= \frac{W_\mathrm{e}}{\mathrm{Vol}} = \frac{\int_0^Q V_\mathrm{C}\,\mathrm{d}Q}{x_0 y_{0,\mathrm{e}} z_0} = \frac{\int_0^{V_\mathrm{C}} C V_\mathrm{C}\,\mathrm{d}V_\mathrm{C}}{x_0 y_{0,\mathrm{e}} z_0} \\ &= \frac{1}{2}\frac{C}{x_0 y_{0,\mathrm{e}}}\frac{V_\mathrm{C}^2}{z_0} = \frac{1}{2}\frac{C}{A_0}\frac{V_\mathrm{C}^2}{z_0} \end{aligned} \tag{17}$$

where $y_{0,\mathrm{e}}$ is the width of the prestretched electrodes, A_0 their area, Q their stored electric charge and V_C the steady-state voltage applied on the actuator equivalent capacitance C (assumed as time-invariant), defined and calculated as specified in Section 3.5;

$$w_\mathrm{m} = \frac{W_\mathrm{m}}{\mathrm{Vol}} = \frac{\int_{x_0}^{x} F_x\,\mathrm{d}x}{x_0 y_{0,\mathrm{e}} z_0} \tag{18}$$

where $F_x = (\text{isotonic stress}_{xx}) y_{0,\mathrm{e}} z_0$ is the active isotonic transverse force, proportional to E_z^2 (Eq. (11)).

The following considerations show how w_m can be easily calculated. Since the active isotonic transverse strain along x is 1/2 of the absolute value of the active isotonic strain along z (Eqs. (8) and (10)), we have:

$$x - x_0 = \frac{x_0}{2z_0}|z - z_0| \tag{19}$$

As $x_0 \gg z_0$, we have $|z - z_0| \ll (x - x_0)$ (from Eq. (19)), so we can neglect the variation of the electric field, and consequently of F_x, with respect to the variation of x:

$$E_z = \frac{V}{z} \cong \frac{V}{z_0} \tag{20}$$

Therefore, we can write:

$$w_\mathrm{m} \cong \frac{F_x}{y_{0,\mathrm{e}} z_0}\frac{x - x_0}{x_0} = (\text{isotonic stress}_{xx})(\text{isotonic strain}_{xx}) \tag{21}$$

Finally, considering the equality of the stress expressions in isotonic and isometric condition (Eqs. (11) and (15)) and assuming Eq. (20) to be valid for both isotonic and isometric conditions (so the stress equality is also numerical, for the same electric field), we have:

$$w_\mathrm{m} \cong (\text{isometric stress}_{xx})(\text{isotonic strain}_{xx}) \tag{22}$$

This means that w_m can be estimated as the product between the measured isometric transverse stress and isotonic transverse strain.

3.5. Calculation of the stored charge and equivalent capacitance

Since the actuator showed imperfect electrodes and dielectric losses (as it will be presented in Sections 4.1 and 4.3, respectively), it was assumed for the device an electrical schematisation consisting of the series between a resistance R_1 and the parallel of a resistance R_2 with a capacitance C, defined as the actuator equivalent capacitance.

Values of C for the four electrode materials, for the four transverse prestresses and for different excitation voltages were calculated by:

$$C = \frac{Q}{V_\mathrm{C}} = \frac{1}{V_\mathrm{C}}\int_{t_1}^{t_2} I_\mathrm{C}(t)\,\mathrm{d}t \tag{23}$$

where t_1 and t_2 are the initial and final stimulation time respectively. $I_\mathrm{C}(t)$, representing the charging current of C, can be calculated as follows:

$$I_\mathrm{C}(t) = I(t) - \frac{V_{R_2}(t)}{R_2} \tag{24}$$

where

$$V_{R_2}(t) = V - R_1 I(t) \tag{25}$$

By observing that R_1 and $R_1 + R_2$ are the equivalent resistances respectively at $t = t_1^+$ (when C is still discharged) and $t = t_2$ (when the dc electrical steady state is fully reached, as it will be shown in Section 4.3), we have that R_1 and R_2 can be easily obtained as:

$$R_1 = \frac{V}{I(t_1^+)} \tag{26}$$

$$R_2 = \frac{V_C}{I(t_2)} \tag{27}$$

Finally, the steady-state voltage on C can be derived as:

$$V_C = V_{R_2}(t_2) \tag{28}$$

4. Results

4.1. Electrode resistance

Unloaded actuators showed an electrode resistance per unit length of 15 kΩ/cm for thickened electrolyte solution electrodes, 50 kΩ/cm for carbon grease, 80 kΩ/cm for graphite powder (inside regions with high particle densities) and 20 kΩ/cm for graphite spray.

4.2. Transverse strain and transverse stress

For thickened electrolyte solution, carbon grease and graphite powder electrodes the isotonic transverse strain and isometric transverse stress (peak values) depended on the square of the applied electric field, for each prestress value:

$$\text{transverse strain} = \beta_S E_z^2 \tag{29}$$

$$\text{transverse stress} = \beta_T E_z^2 \tag{30}$$

As an example, Fig. 5a and b shows this trend for one electrode material and for all the tested prestresses.

For graphite spray electrodes a saturation effect was observed for each prestress value (Fig. 6a and b), as expected for dielectric polymers [11], possibly due to the dielectric nonlinearity of the polymer. This trend was most evident for graphite spray electrodes, because they allowed the application of the highest electric fields (Tables 2 and 3), enabling the manifestation of the saturation.

A comparison of the strain–field curves related to the different electrode materials, for each definite prestress, is presented by Fig. 7a–d.

Tables 2 and 3 list, for the different electrode materials and prestresses, β_S and β_T (calculated by data fitting[3]), the maximum recorded values of isotonic transverse strain and isometric transverse stress, and a range including the electric field causing the dielectric breakdown (E_{break}) in isotonic and isometric condition.

The two images of Fig. 8 show an example of transverse displacement during actuation.

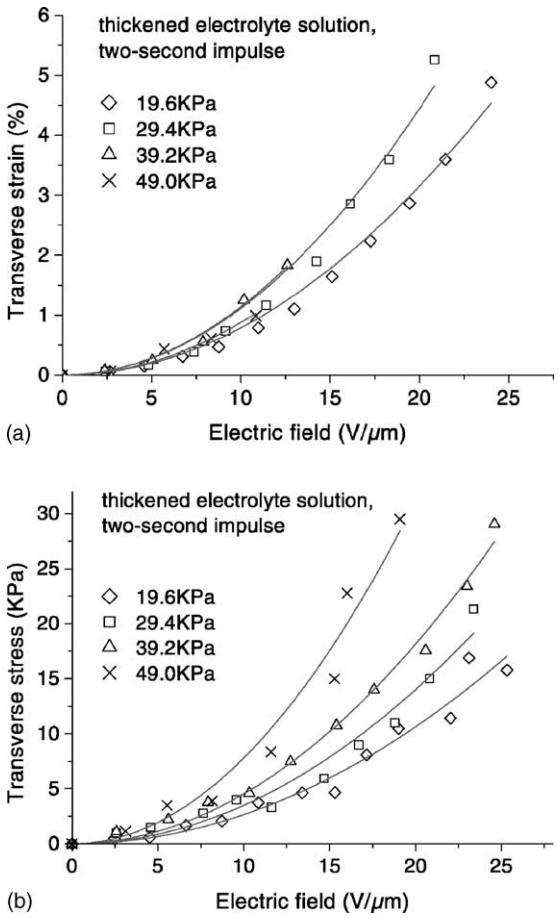

Fig. 5. Peak isotonic transverse strain (a) and isometric transverse stress (b) vs. electric field for thickened electrolyte solution electrodes and different prestresses (the legend symbols indicate different prestresses).

4.3. Driving current

Regardless of the electrode material and prestress, in isotonic condition each measured driving current signal showed an initial peak ($I(t_1^+) = I_p$), followed by a fast exponential decrease towards a nonzero asymptotic value (see the example of Fig. 9). These signals demonstrate that the dc electrical steady state was reached at the end of the 2 s stimulation.

Moreover, the lack of a zero setting of the steady-state current suggests the presence of dielectric losses inside the polymer.

At "low" electric fields E_z the peak current per unit electrode area (I_p/A_0) was found, for each prestress, to be basi-

[3] In order to allow a strain and stress numerical comparison among all the different electrode materials, the data fitting based on Eqs. (29) and (30) was performed also for graphite spray electrodes at low electric fields (see the indications reported in Tables 2 and 3).

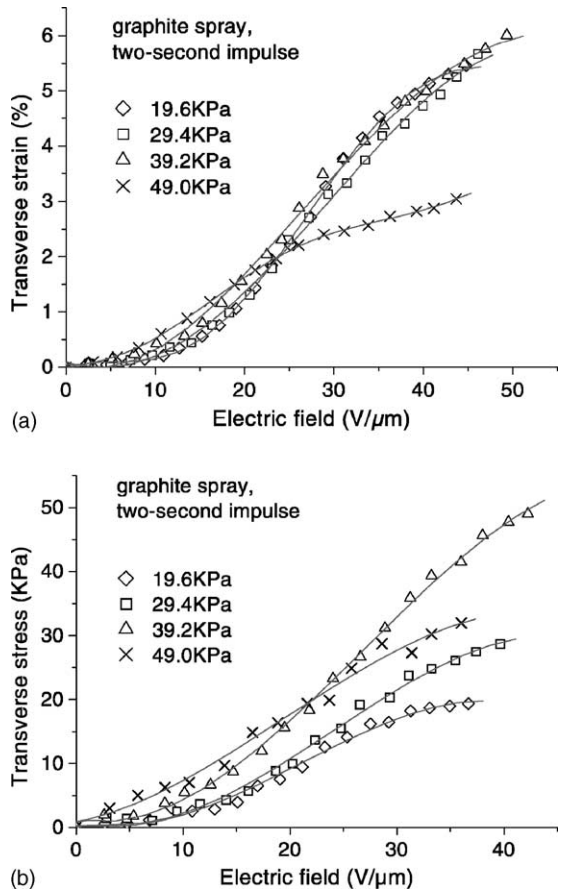

Fig. 6. Peak isotonic transverse strain (a) and isometric transverse stress (b) vs. electric field for graphite spray electrodes and different prestresses.

cally in direct proportion to E_z (see Fig. 10a as an example):

$$\frac{I_p}{A_0} = \alpha_I E_z \tag{31}$$

A tendency to saturation was observed at high electric fields. This phenomenon was most evident for graphite spray electrodes (and particularly for a prestress of 49.0 kPa, as shown by Fig. 10b), since it was made visible by the highest dielectric strength enabled by these electrodes.

Table 4 lists values of α_I (calculated as initial slope of the data fitting curves) and of the maximum recorded I_p/A_0 for the tested electrode materials and prestresses.

4.4. Stored charge and equivalent capacitance

For each electrode material and prestress, the calculated stored charge per unit electrode area (Q/A_0) resulted substantially linearly dependent on the applied electric field (see Fig. 11a as an example):

$$\frac{Q}{A_0} = \alpha_Q E_z \tag{32}$$

while the equivalent capacitance per unit electrode area (C/A_0) showed basically constant values (Fig. 12a).

One exception was revealed by graphite spray electrodes with a prestress of 49.0 kPa: the related Q/A_0 and C/A_0 plots versus E_z presented a fitting curve with decreasing slope at high electric fields (Figs. 11b and 12b), as predictable consequence of the saturation shown by the measured current (Fig. 10b).

Table 2
Isotonic transverse strain

Electrode material	Transverse prestress (kPa)	β_S (%/(V/μm)^2)	Maximum transverse strain (%)[a]	Isotonic E_{break} (V/μm)[a]
Thickened electrolyte solution	19.6	7.9×10^{-3}	4.9 @ 24 V/μm	24–27
	29.4	11.1×10^{-3}	5.3 @ 21 V/μm	21–24
	39.2	11.4×10^{-3}	1.8 @ 13 V/μm	13–16
	49.0	8.8×10^{-3}	1.0 @ 11 V/μm	11–14
Carbon grease	19.6	3.2×10^{-3}	4.3 @ 34 V/μm	34–37
	29.4	3.7×10^{-3}	5.2 @ 38 V/μm	38–41
	39.2	4.5×10^{-3}	2.3 @ 22 V/μm	22–25
	49.0	3.5×10^{-3}	2.3 @ 24 V/μm	24–27
Graphite powder	19.6	3.9×10^{-3}	5.6 @ 37 V/μm	37–40
	29.4	3.4×10^{-3}	3.6 @ 31 V/μm	31–34
	39.2	2.3×10^{-3}	1.7 @ 26 V/μm	26–29
	49.0	1.0×10^{-3}	1.0 @ 31 V/μm	31–34
Graphite spray	19.6	3.6×10^{-3} [b]	5.5 @ 45 V/μm	45–48
	29.4	3.5×10^{-3} [b]	5.7 @ 46 V/μm	46–49
	39.2	4.1×10^{-3} [c]	6.0 @ 49 V/μm	49–52
	49.0	4.8×10^{-3} [d]	3.0 @ 44 V/μm	44–47

[a] For a 2 s voltage impulse.
[b] Quadratic fitting up to 31 V/μm.
[c] Quadratic fitting up to 29 V/μm.
[d] Quadratic fitting up to 16 V/μm.

Table 3
Isometric transverse stress

Electrode material	Transverse prestress (kPa)	β_T (kPa/(V/μm)^2)	Maximum transverse stress (kPa)[a]	Isometric E_{break} (V/μm)
Thickened electrolyte solution	19.6	26.6×10^{-3}	16.9 @ 23 V/μm	23–26
	29.4	35.1×10^{-3}	21.3 @ 23 V/μm	23–26
	39.2	45.4×10^{-3}	29.0 @ 25 V/μm	25–28
	49.0	78.1×10^{-3}	29.5 @ 19 V/μm	19–22
Carbon grease	19.6	16.6×10^{-3}	17.2 @ 33 V/μm	33–36
	29.4	23.3×10^{-3}	29.2 @ 33 V/μm	33–36
	39.2	30.5×10^{-3}	23.2 @ 27 V/μm	27–30
	49.0	49.7×10^{-3}	29.0 @ 24 V/μm	24–27
Graphite powder	19.6	16.0×10^{-3}	18.4 @ 37 V/μm	37–40
	29.4	17.8×10^{-3}	31.0 @ 42 V/μm	42–45
	39.2	32.9×10^{-3}	42.9 @ 35 V/μm	35–38
	49.0	24.0×10^{-3}	31.2 @ 39 V/μm	39–42
Graphite spray	19.6	21.8×10^{-3} [b]	19.3 @ 37 V/μm	37–40
	29.4	25.4×10^{-3} [c]	28.7 @ 40 V/μm	40–43
	39.2	40.2×10^{-3} [c]	49.0 @ 42 V/μm	42–45
	49.0	56.5×10^{-3} [d]	32.0 @ 36 V/μm	36–39

[a] For a 2 s voltage impulse.
[b] Quadratic fitting up to 23 V/μm.
[c] Quadratic fitting up to 22 V/μm.
[d] Quadratic fitting up to 16 V/μm.

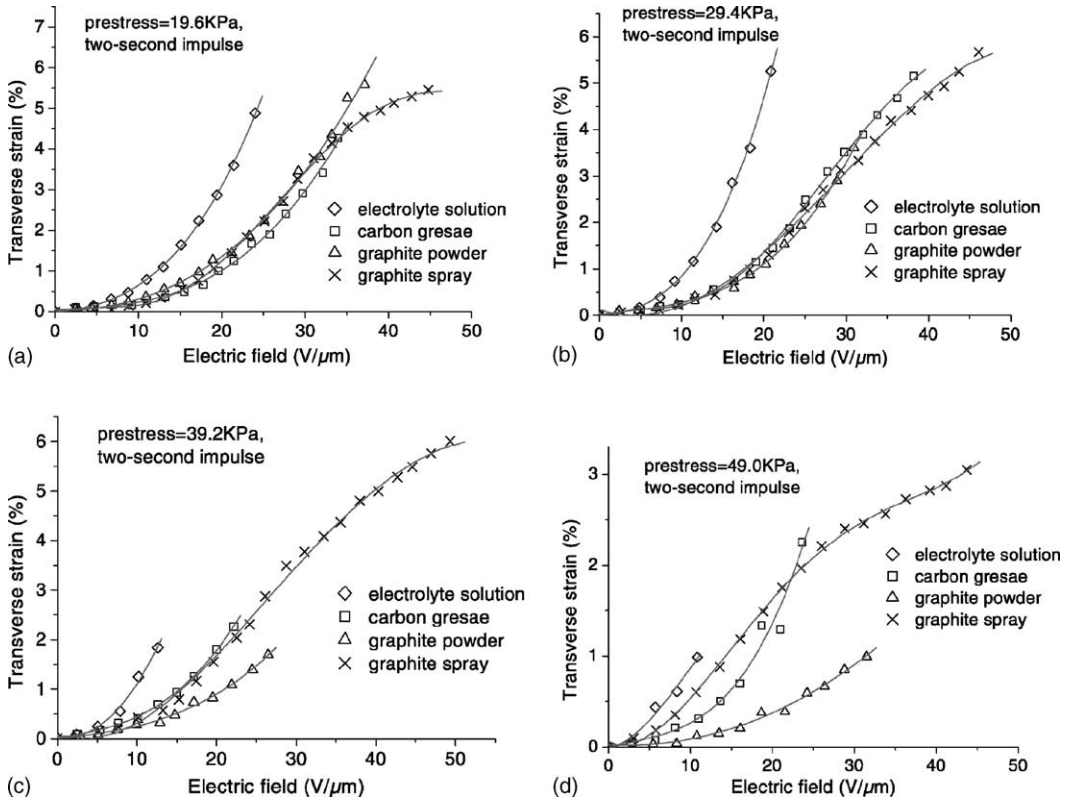

Fig. 7. Peak isotonic transverse strain vs. electric field for the different electrode materials and a prestress of 19.6 kPa (a), 29.4 kPa (b), 39.2 kPa (c) and 49.0 kPa (d).

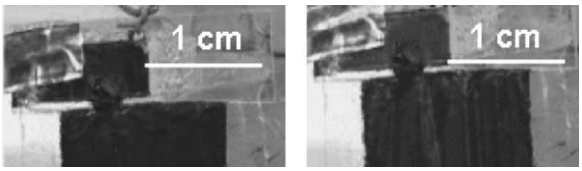

Fig. 8. Electrically induced isotonic transverse displacement of the upper end of an actuator with carbon grease electrodes (black area).

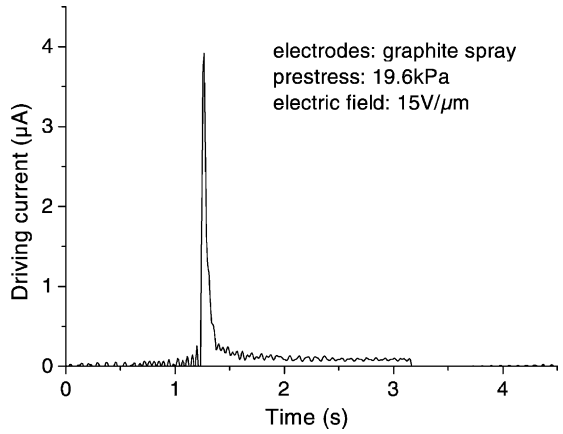

Fig. 9. A measured driving current signal. This trend was common to all the detected signals.

Table 4
Driving current in isotonic actuation

Electrode material	Transverse prestress (kPa)	α_I ((μA/cm^2)/(V/μm))	Maximum I_p/A_0 (μA/cm^2)
Thickened electrolyte solution	19.6	0.87×10^{-1}	2.0 @ 24 V/μm
	29.4	0.87×10^{-1}	1.9 @ 21 V/μm
	39.2	1.45×10^{-1}	2.0 @ 13 V/μm
	49.0	1.69×10^{-1}	2.0 @ 11 V/μm
Carbon grease	19.6	0.41×10^{-1}	1.5 @ 34 V/μm
	29.4	0.67×10^{-1}	2.1 @ 38 V/μm
	39.2	0.80×10^{-1}	1.6 @ 22 V/μm
	49.0	1.37×10^{-1}	2.9 @ 24 V/μm
Graphite powder	19.6	0.69×10^{-1}	2.9 @ 37V/μm
	29.4	0.48×10^{-1}	1.5 @ 31 V/μm
	39.2	0.59×10^{-1}	1.4 @ 26 V/μm
	49.0	0.37×10^{-1}	1.3 @ 31 V/μm
Graphite spray	19.6	0.72×10^{-1}	2.9 @ 43 V/μm
	29.4	0.80×10^{-1}	3.2 @ 46 V/μm
	39.2	0.96×10^{-1}	3.5 @ 49 V/μm
	49.0	1.41×10^{-1}	3.8 @ 36 V/μm

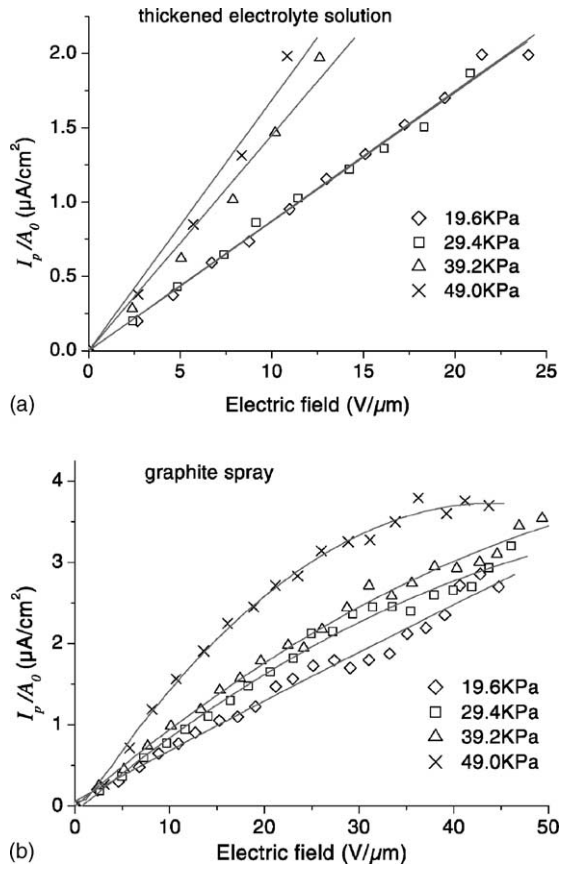

Fig. 10. Peak current per unit electrode area (I_p/A_0) vs. electric field for thickened electrolyte solution (a) and graphite spray (b) electrodes and different prestresses.

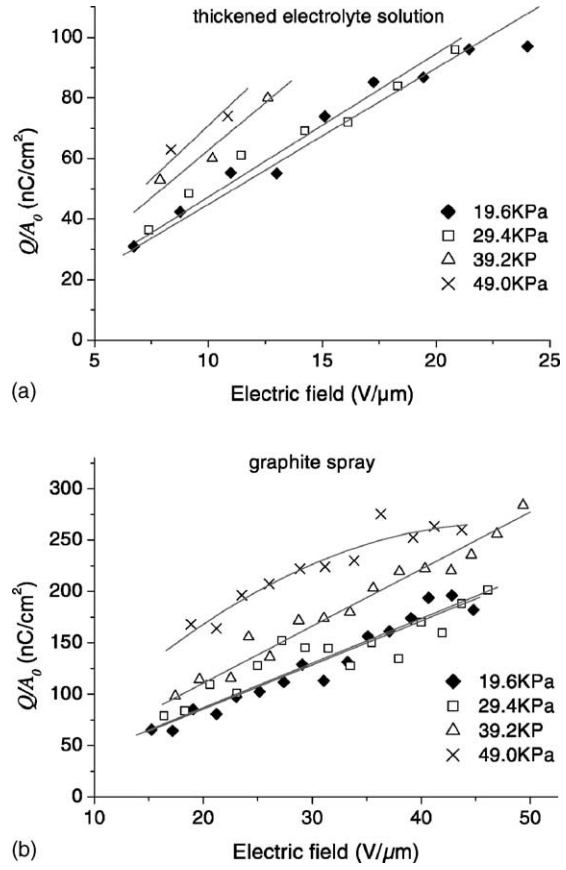

Fig. 11. Stored charge per unit electrode area (Q/A_0) vs. electric field for thickened electrolyte solution (a) and graphite spray (b) electrodes and different prestresses.

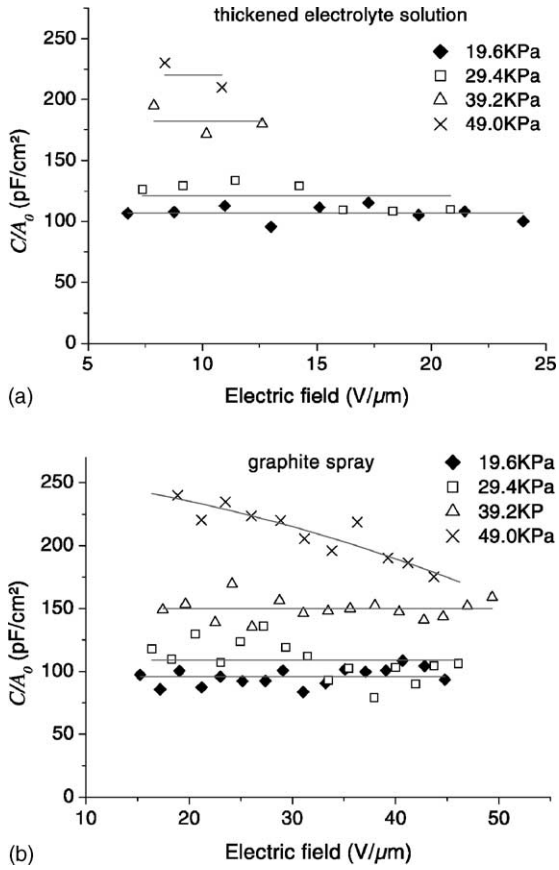

Fig. 12. Equivalent capacitance per unit electrode area (C/A_0) vs. electric field for thickened electrolyte solution (a) and graphite spray (b) electrodes and different prestresses.

Values of α_Q (calculated by data fitting), of the maximum recorded Q/A_0 and of the average C/A_0 for the different electrode materials and prestresses are presented in Table 5.

Table 6
Efficiency

Electrode material	Transverse prestress (kPa)	Maximum efficiency (%)[a]
Thickened electrolyte solution	19.6	9 @ 24 V/μm
	29.4	10 @ 21 V/μm
	39.2	3 @ 13 V/μm
	49.0	2 @ 11 V/μm
Carbon grease	19.6	4 @ 34 V/μm
	29.4	6 @ 34 V/μm
	39.2	3 @ 22 V/μm
	49.0	3 @ 24 V/μm
Graphite powder	19.6	4 @ 35 V/μm
	29.4	5 @ 31 V/μm
	39.2	3 @ 26 V/μm
	49.0	2 @ 31 V/μm
Graphite spray	19.6	4 @ 31 V/μm
	29.4	4 @ 35 V/μm
	39.2	5 @ 38 V/μm
	49.0	–

[a] For a 2 s voltage impulse.

4.5. Electromechanical coupling efficiency

Eqs. (16), (17) and (22) show that the theoretical electromechanical coupling efficiency depends on the square of the applied electric field (w_m depends on E_z^4, while w_e on E_z^2). This trend was confirmed by the efficiency calculated from experimental data for thickened electrolyte solution, carbon grease and graphite powder electrodes. For graphite spray electrodes the efficiency showed a field dependence similar to that of the strain and stress up to the beginning of their saturation, which caused a subsequent predictable decrease of the efficiency.

Maximum values of the electromechanical coupling efficiency are reported in Table 6.

Table 5
Stored charge and equivalent capacitance in isotonic actuation

Electrode material	Transverse prestress (kPa)	α_Q ((nC/cm^2)/(V/μm))	Maximum Q/A_0 (nC/cm^2)	Average C/A_0 (pF/cm^2)
Thickened electrolyte solution	19.6	4.5	97 @ 24 V/μm	107
	29.4	4.7	96 @ 21 V/μm	121
	39.2	6.3	80 @ 13 V/μm	182
	49.0	7.1	74 @ 11 V/μm	220
Carbon grease	19.6	3.5	114 @ 34 V/μm	81
	29.4	3.6	129 @ 38 V/μm	85
	39.2	5.4	112 @ 22 V/μm	115
	49.0	5.9	140 @ 24 V/μm	138
Graphite powder	19.6	4.3	161 @ 37 V/μm	96
	29.4	3.2	109 @ 31 V/μm	83
	39.2	3.1	85 @ 26 V/μm	85
	49.0	3.3	108 @ 31 V/μm	92
Graphite spray	19.6	4.3	196 @ 43 V/μm	96
	29.4	4.3	202 @ 46 V/μm	109
	39.2	5.5	284 @ 49 V/μm	150
	49.0	–	275 @ 36 V/μm	–

5. Discussion

5.1. Effect of the different electrode materials on active strain

Fig. 7a–d and Table 2 show that, for each prestress and electric field, the different electrode materials allow the generation of different strains.

These unequal performances could be interpreted in terms of an unequal amount of charge stored (in isotonic actuation) by the unit area of the different electrodes, enabling different values of "useful" electric field, as proposed below.

By applying a certain voltage V across the definite thickness z_0 of a prestreched actuator, the resulting electrostatic pressure generates a strain depending on the square of the applied electric field. For an ideal device with electrodes made of a perfect conductor (electrical resistance equal to zero) this field would be V/z_0. Contrarily, the tested electrodes and elastomer showed a lack of both electric and dielectric ideality (see Sections 4.1 and 4.3, respectively), so that we could take into account an effective electric field, different from the nominal one used so far (V/z_0). In particular, we could consider as "useful" electric field ($E_{z,\mathrm{u}}$) the one calculated by applying the Gauss' law to an imaginary closed surface (S, with orthogonal versor $\vec{n}$) surrounding one of the two electrodes:

$$\oiint_S \vec{E}_{z,\mathrm{u}} \cdot \vec{n}\, \mathrm{d}S = \frac{Q}{\varepsilon_0 \varepsilon_\mathrm{r}} \Rightarrow E_{z,\mathrm{u}} = \frac{Q}{A_0 \varepsilon_0 \varepsilon_\mathrm{r}} \tag{33}$$

This equation shows that $E_{z,\mathrm{u}}$ increases by increasing the charge stored by the unit area of the electrodes Q/A_0.

The presented experimental data agree with the prediction enabled by the previous simple remark for each prestress and substantially each nominal electric field. In fact, for each prestress the ordering, among the different electrode materials, of the measured strains (see values of β_S in Table 2) reflects substantially the same ordering of the calculated Q/A_0 (see values of α_Q in Table 5).

5.2. Effect of the different prestress values on active strain

Results showed that, for each electrode material and for the same nominal electric field, the prestress increase up to 39.2 kPa improved the actuator strain (see values of β_S in Table 2).

Following the interpretation proposed in Section 5.1, this could be ascribed to a raising amount of charge stored by the unit electrode area for the increasing prestresses.

This is consistent with the experimental data, as can be found from the comparison of values of β_S (Table 2) and α_Q (Table 5).

An unpredictable behaviour was observed for a prestress of 49.0 kPa for all the tested electrode materials, even though for graphite spray electrodes the bending of the strain–field curve after 20 V/μm (Fig. 6a) agrees with that of the Q/A_0–field curve (Fig. 11b).

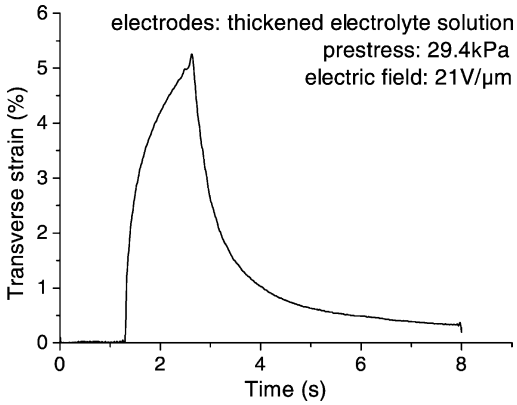

Fig. 13. Example of isotonic transverse strain signal.

5.3. Effects of different voltage impulse lengths

The electromechanical performances reported in this article have to be considered as strictly dependent on the duration (2 s) of the applied voltage impulse. In fact, this value, chosen (arbitrarily) for the comparisons presented here, did not allow the actuator to reach its mechanical equilibrium (Fig. 13).

Consequently, performances were not optimised, since they could be higher for longer impulses. However, performance optimisation goes beyond the aims of this study.

6. Conclusions

The electromechanical performances of dielectric elastomer planar actuators largely depended on the electrode material and prestress value.

The presented data allow one to select, for different ranges of electric field, suitable electrode material and prestress (among those tested), to realise actuators able to show the best strain, stress or efficiency. Briefly, thickened electrolyte solution electrodes were best for most purposes for electric fields up to 20–25 V/μm (and opportune prestress values), above which graphite spray electrodes were generally optimal.

An interpretation of the strain capabilities in isotonic condition was proposed in terms of the amount of charge stored by the unit electrode area, which is a key feature to maximise for the design of future high performance electrodes.

References

[1] D. De Rossi, M. Suzuki, Y. Osada, P. Morasso, Pseudo-muscular gel actuators for advanced robotics, J. Intell. Mater. Syst. Struct. 3 (1992) 75–95.
[2] A. Della Santa, D. De Rossi, A. Mazzoldi, Performances and working capacity of a PPy conducting polymer linear actuator, Synth. Met. 90 (1997) 93–100.
[3] T. Ueda, et al., Polyurethane elastomer actuator, Synth. Met. 85 (1997) 1415–1416.

[4] Q.M. Zhang, V. Bharti, X. Zhao, Giant electrostriction and relaxor ferroelectric behaviour in electron-irradiated poly(vinylidene fluoride-trifluoroethylene) copolymer, Science 280 (1998) 2101–2103.
[5] R.H. Baughman, et al., Carbon nanotube actuators, Science 284 (1999) 1340–1344.
[6] E.W. Jager, E. Smela, O. Inganas, Microfabricating conjugated polymer actuators, Science 290 (2000) 1540–1545.
[7] Y. Bar-Cohen, Electroactive Polymer (EAP) Actuators as Artificial Muscles—Reality, Potential and Challenges, vol. 8, SPIE Press, Washington, 2001, p. 23.
[8] R. Perline, R. Kohrnbluh, Q. Pei, J. Joseph, High-speed electrically actuated elastomers with strain greater than 100%, Science 287 (2000) 836–839.
[9] R.E. Pelrine, R.D. Kornbluh, J.P. Joseph, Electrostriction of polymer dielectrics with compliant electrodes as a means of actuation, Sens. Actuators, A 64 (1998) 77–85.
[10] R. Heydt, R. Kohrnbluh, R. Perline, V. Mason, Design and performance of an electrostrictive-polymer-film acoustic actuator, J. Sound Vib. 215 (2) (1998) 297–311.
[11] Y. Bar-Cohen, Electroactive Polymer (EAP) Actuators as Artificial Muscles—Reality, Potential and Challenges, vol. 93, SPIE Press, Washington, 2001, p. 429.

Biographies

Federico Carpi graduated in electronic engineering at the University of Pisa in 2001. He is a PhD student in bioengineering at the University of Pisa. He works on polymer actuators for biomedical engineering and robotics. He is author of several contributions to international conferences and chapters in international books.

Piero Chiarelli graduated in physics at the University of Pisa in 1982. In 1988, he became researcher of the Institute of Clinical Physiology of C.N.R. He worked in USA, Japan, Germany and Hungary. Presently he teaches biomedical instrumentation at the University of Pisa. His scientific activities are related to the electro-mechano-chemical kinetics of polymer gels, to the dynamics of bi-phase materials and biological tissues, and to the design of sensors and actuators for bioengineering and robotics. He is author of over 80 technical and scientific publications.

Alberto Mazzoldi graduated in chemical engineering at the University of Pisa in 1993. He took the PhD degree in bioengineering in 1998. From 2000, he is researcher at the School of Engineering of the University of Pisa. His main scientific interests concern actuators for biomedical and robotic applications. He is author of about 50 technical and scientific publications.

Danilo De Rossi graduated in chemical engineering at the University of Genova in 1976. From 1976 to 1981, he was researcher of the Institute of Clinical Physiology of C.N.R. He worked in France, USA, Brasil and Japan. Since 1982, he has been working in the School of Engineering of the University of Pisa, where presently he is full professor of bioengineering. His scientific activities are related to the physics of organic and polymeric materials, and to the design of sensors and actuators for bioengineering and robotics. He is author of over 150 technical and scientific publications.